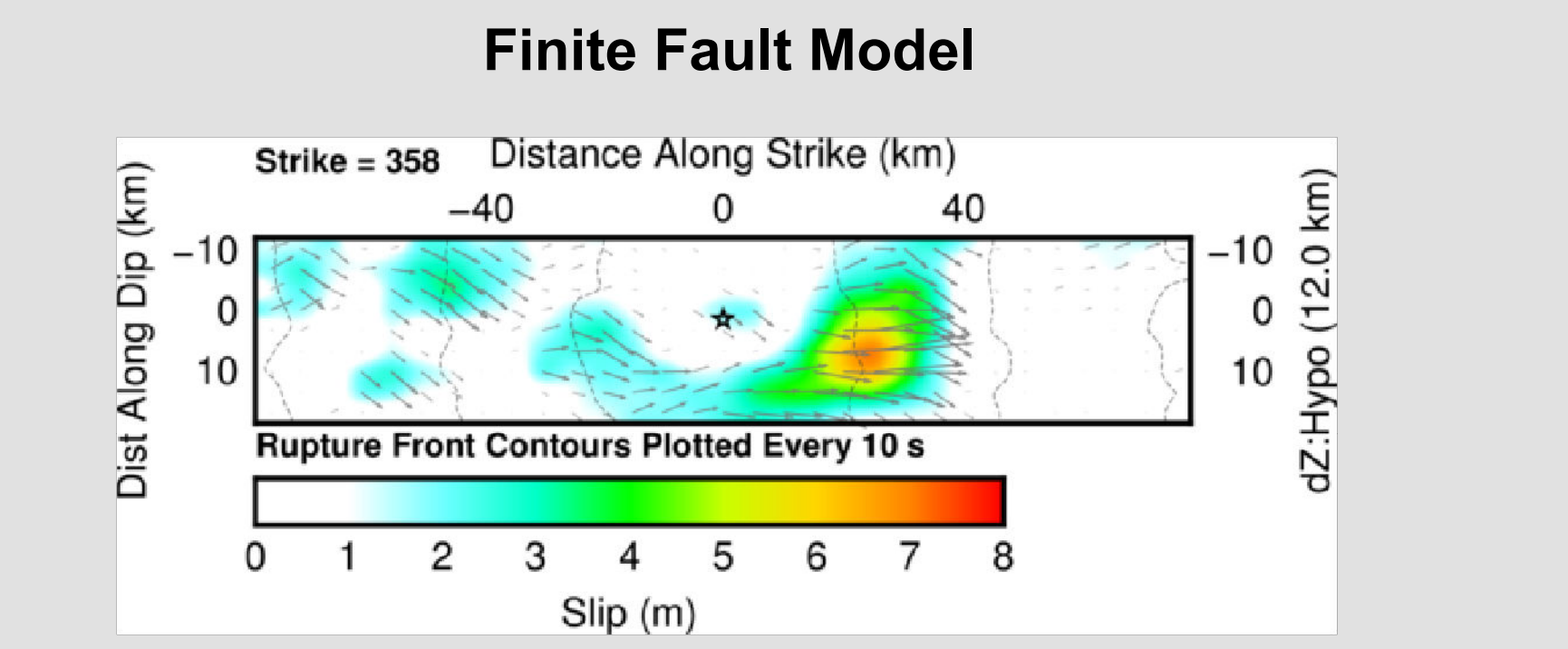
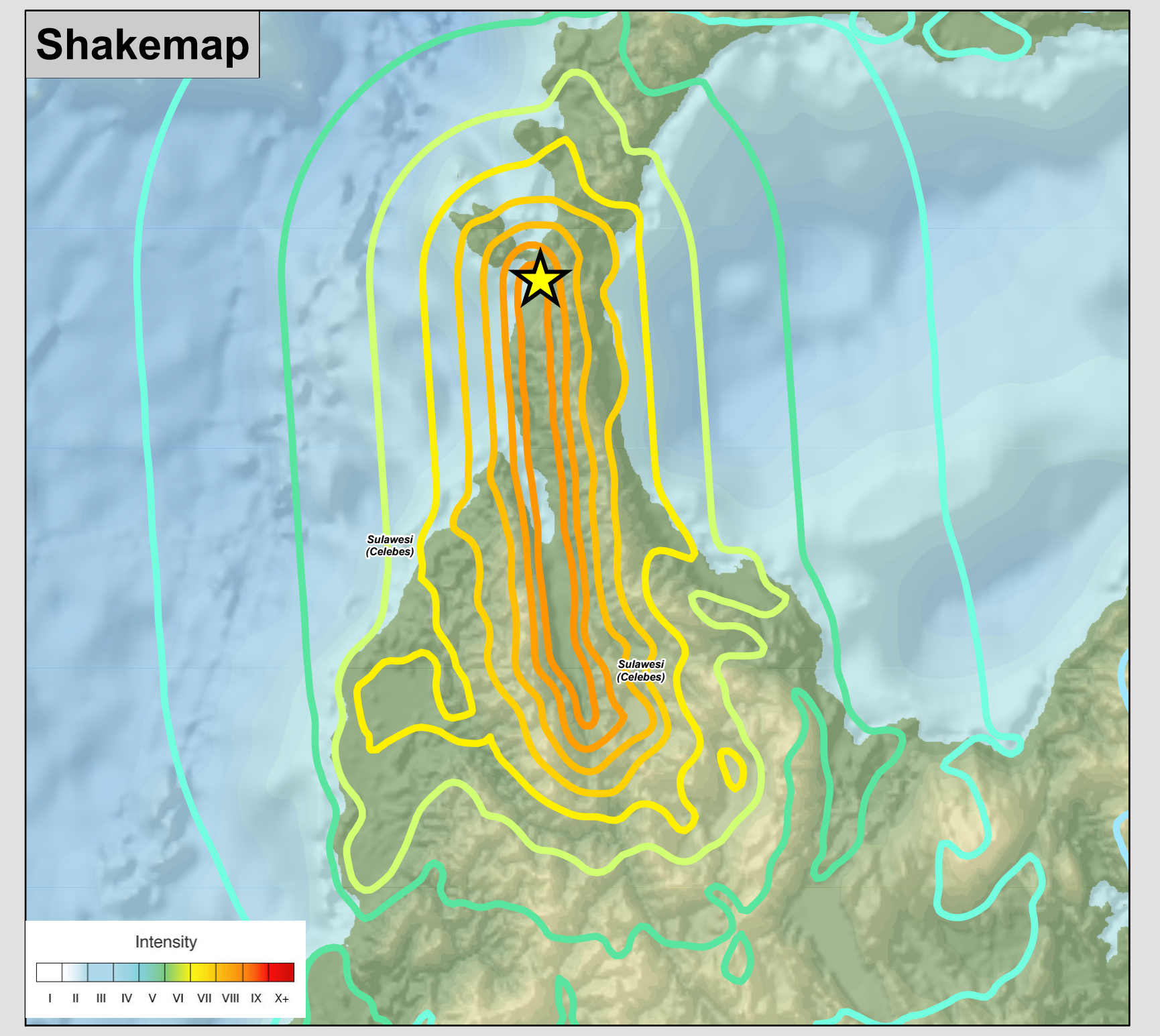


Tectonic Summary

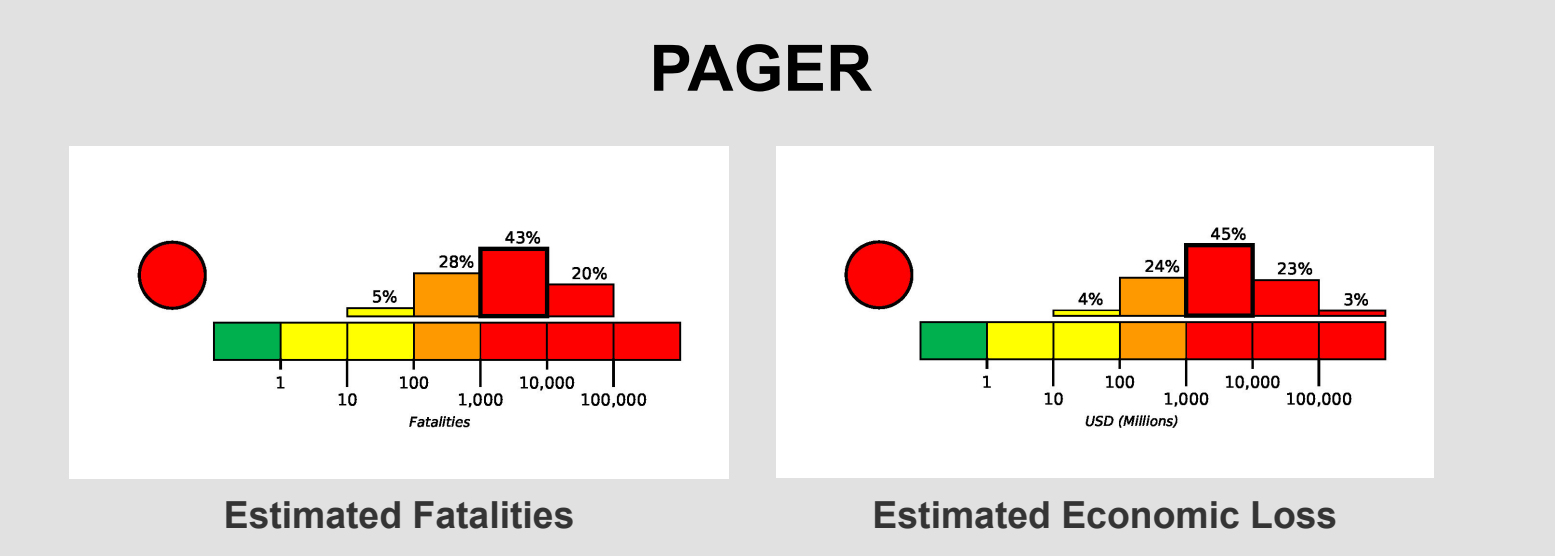
The September 28, 2018, M 7.5 earthquake near Sulawesi, Indonesia occurred as a result of strike-slip faulting at shallow depths within the interior of the Molucca Sea microplate, part of the broader Sunda tectonic plate. Focal mechanism solutions for the earthquake indicate rupture occurred on either a left-lateral north-south striking fault, or along a right-lateral east-west striking fault. Eastern Indonesia is characterized by complex tectonics in which motions of numerous small microplates are accommodating large-scale convergence between the Australia, Sunda, Pacific, and Philippine Sea plates. At the location of the September 28th earthquake, the Sunda plate moves south with respect to Molucca Sea plate at a velocity of about 30 mm/year.

While commonly plotted as points on maps, earthquakes of this size are more appropriately described as slip over a larger fault area. Strike-slip events of the size of the September 28, 2018 earthquake are typically about 120x20 km in size (length x width); modeling of this earthquake implies dimensions of ~80x30 km, predominantly down-dip and south of the hypocenter.

Shallow earthquakes of this size can often have a deadly impact on nearby communities. Historically, this region has hosted several large earthquakes, with fifteen events of M 6.5 and larger within 250 km of the September 28th earthquake over the preceding century. The largest of these was a M 7.9 earthquake in January 1996, about 100 km to the north of the September 28, 2018 event. The 1996 earthquake – a shallow thrust faulting earthquake likely to have occurred on the regional subduction zone system at depth beneath the shallow crust – resulted in approximately 10 fatalities, over 60 injuries, and significant building damage in the local region. The September 28, 2018 earthquake was preceded by a series of small-to-moderate sized earthquakes over the hours leading up to this event; the USGS located 4 other earthquakes of M 4.9 and larger in the epicentral region, beginning with a M 6.1 earthquake three hours earlier and just to the south of the M 7.5 event. There has also been an active aftershock sequence, with ten events of M 4.7 and larger in the three hours following this earthquake. The largest aftershock in this timeframe was M 5.8, about 12



Distribution of the amplitude and direction of slip for subfault elements of the fault rupture model are determined from the inversion of teleseismic body waveforms and long period surface waves. Arrows indicate the amplitude and direction of slip (of the hanging wall with respect to the foot wall); the slip is also colored by magnitude. The view of the rupture plane is from above. The strike of the fault rupture plane is 358° and the dip is 86° N. The dimensions of the subfault elements are 5 km in the strike direction and 3.4 km in the dip direction. The rupture surface is approximately 40 km along strike and 20 km along down-dip. The seismic moment release based upon this plane is 2.0e+27 dyne-cm.

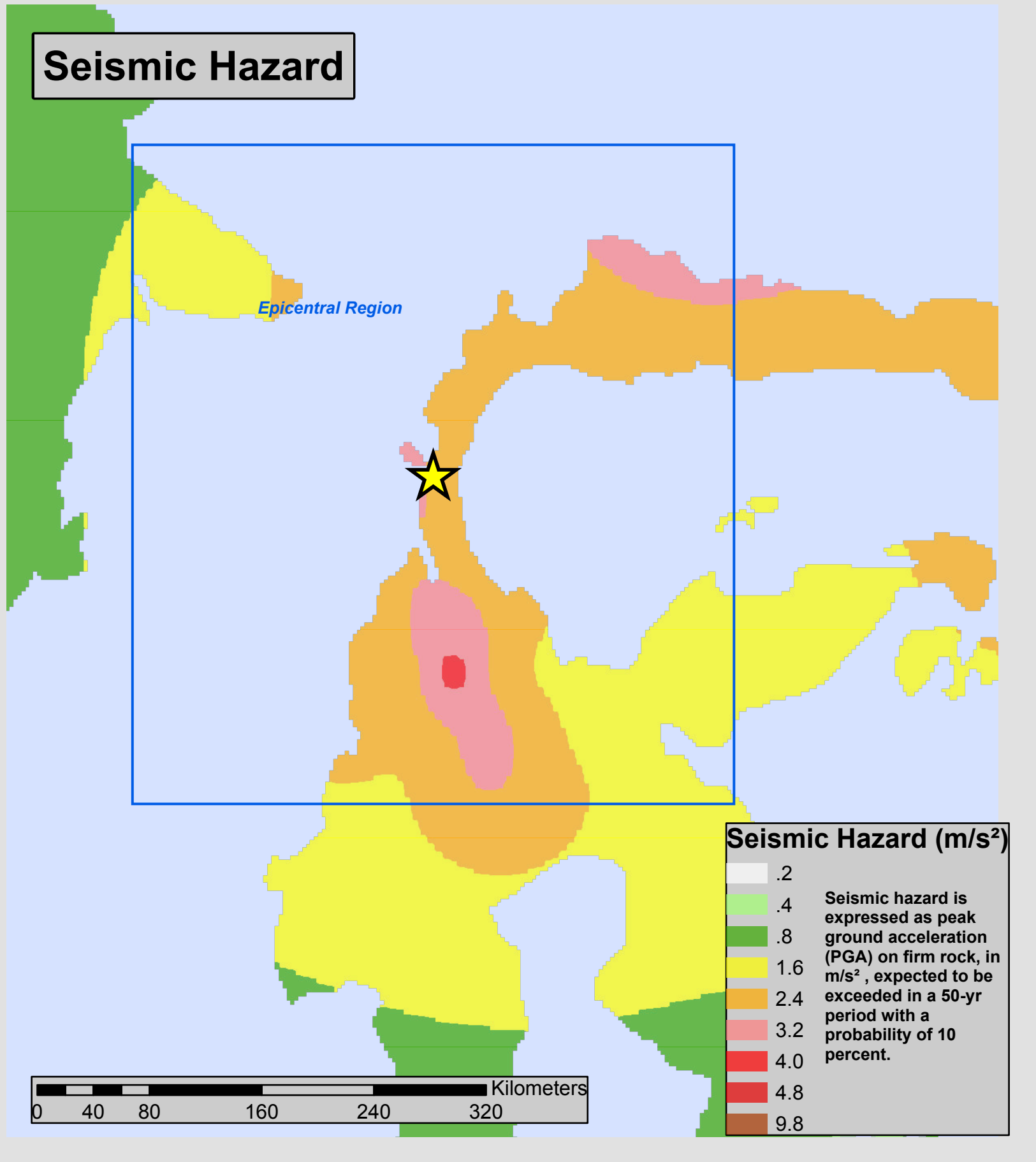


Cities Exposed to Shaking

Shaking	City	Population
IX	Palu	202k
VIII	Sigi Biromaru	0k
VII	Donggala	0k
VI	Parigi	0k
VI	Kastiguncu	0k
V	Tobadak	0k
IV	Mamuju	15k
IV	Samarinda	355k
IV	Makassar	1,322k
IV	Gorontalo	144k
IV	Kendari	195k

Population Exposed to Shaking

Shaking	Population
I Not Felt	0k*
II-III Weak	6,453k*
IV Light	14,331k
V Moderate	1,175k
VI Strong	416k
VII Very Strong	147k
VIII Severe	402k
IX Violent	422k
X Extreme	0k



DATA SOURCES

EARTHQUAKES AND SEISMIC HAZARD
USGS, National Earthquake Information Center
NOAA, National Geophysical Data Center
IASPEI Centennial Catalog (1900 - 1999) and extensions (Engdahl and Villasefor, 2002)
EHB catalog (Engdahl et al., 1998)
HDF (unpublished earthquake catalog, Engdahl, 2003)
Global Seismic Hazard Assessment Program
Volcanoes of the World (Siebert and Simkin, 2002)

PLATE TECTONICS AND FAULT MODEL
PB2002 (Bird, 2003)
Ji, C., D.J. Wald, and D.V. Helmlinger, Source description of the 1999 Hector Mine, California earthquake, Part I: Wavelet domain inversion theory and resolution analysis, Bull. Seism. Soc. Am., Vol 92, No. 4, pp. 1192-1207, 2002.
Delilets, C., Gordon, R.G., Argus, D.F., 2010. Geologically current plate motions, Geophys. J. Int. 181, 1-80.

BASE MAP
NIMA and ESRI, Digital Chart of the World
USGS, EROS Data Center
NOAA GEBCO and GLOBE Elevation Models

REFERENCES

Bird, P., 2003, An updated digital model of plate boundaries: Geochim. Geophys. Geosyst., v. 4, no. 3, pp. 1027-80.

Engdahl, E.R., and Villasefor, A., 2002, Global Seismicity, 1900-1999, chap. 41 of Lee, W.H.K., and others, eds., International Earthquake and Engineering Seismology, Part A: New York, N.Y., Elsevier Academic Press, 832 p.

Engdahl, E.R., Van der Hilst, R.D., and Buland, R.P., 1998, Global teleseismic earthquake relocation with improved travel times and procedures for depth determination, Bull. Seism. Soc. Amer., v. 88, p. 722-743.

DISCLAIMER

Base map data, such as place names and political boundaries, are the best available but may not be current or may contain inaccuracies and therefore should not be regarded as having official significance.

Map updated by U.S. Geological Survey National Earthquake Information Center
28 September 2018
http://earthquake.usgs.gov/
Map not approved for release by Director USGS